Combinatorial optimization approach for the efficient reuse of RC components

Jannis Rose[1] | **Patrick Forman**[1] | **David Stieler**[2] | **Achim Menges**[2] | **Peter Mark**[1]

[1]Institute of Concrete Structures, Ruhr University Bochum, North Rhine Westphalia, Germany

[2]Institute for Computational Design and Construction, University of Stuttgart, Baden Württemberg, Germany

Correspondence
Jannis Rose
Email: jannis.rose@rub.de

Present address
Ruhr University Bochum
Institute of Concrete Structures
Universitätsstraße 150
44780 Bochum

Abstract

The reuse of reinforced concrete components from deconstructed buildings offers a promising approach to reduce the environmental impact of new constructions. However, it represents a complex combinatorial optimization problem to efficiently place the available modules, which vary in geometry and load-bearing capacity, into new structures while maximizing their utilization. This paper proposes a two-stage optimization method to enable the reuse of arbitrary reinforced concrete modules. First, an agent-based model is employed to rapidly explore feasible geometric combinations of modules and preselect suitable placements based on a target span length. Second, metaheuristic optimization algorithms, namely Simulated Annealing and Tabu Search, are adapted to maximize the utilization of the modules' load-bearing capacity while ensuring global structural integrity. The methods are demonstrated on a case study of assembling a three-span continuous beam from a sampled construction kit of 100 reinforced concrete modules with varying cross-sectional properties and material parameters. The results show the agent-based preselection effectively finds viable geometric combinations, while the metaheuristics converge on optimised module placements with up to 88% utilization on average. The proposed approach provides a computational framework to enable the direct reuse of structural concrete components, supporting the design of low-carbon circular buildings.

KEYWORDS
construction kit, reuse, combinatorial optimization, metaheuristic, reinforced concrete, modular construction, circularity, structural design

1 | INTRODUCTION

For centuries, building has served to fulfill basic needs such as providing shelter, supply, and disposal. The steady population growth results in many new construction projects as well as replacements, while also maintaining existing structures. This has led to a high demand for resources, as well as increased emissions and waste from construction. More precisely, construction activities account for about 20% of global CO_2 emissions[1] and 90% of natural mineral extraction, as well as 35% of waste generation across Europe[2]. Reinforced Concrete (RC) is the dominant building material, resulting in 8-9% of global CO_2 emissions from cement production alone[3]. To reduce the environmental impact of RC buildings, researchers are increasingly exploring alternatives to holistic new construction[4]. Recycling is the most widespread method for reutilizing existing structures at a material level. Through complex dismantling, RC structures are destructively broken down into their name-giving components, concrete and steel reinforcement. Concrete can then be used as an aggregate for so called recycled concrete[5] or as a filler material in road construction. However, this approach does not replace energy-intensive cement production.

A less emitting method is reuse that involves utilizing entire components for new structures in an equivalent manner[6,7], as various studies have shown[8]. This means that the current building stock becomes the component stock or construction kit for future structures. Steel construction, with its inherently modular character and generally bolted connections, already facilitates reuse[9]. Reuse is also increasingly being used for RC components[8,10,11]. Thereby, precast concrete components are particularly suitable for this purpose[12], as they can be easily separated at their regular connections and reused in a quasi-equivalent way, such as prestressed hollow core slabs[13]. Also from monolithic structures, RC components can be separated, for example, by

sawing and become modules for reuse. The cut edges then form the subsequent joints for new structures and must be prepared to transmit forces and moments if necessary. There are two types of joints: classic poured joints and (often pre-stressed) dry joints. Therefore, various types of joints to connect RC components are numerically and experimentally investigated[14,15]. The reuse for concrete components shows, for example, a 10-metre span, prestressed arch bridge[16]. The almost equal RC modules are cut out of an existing structure and then are reassembled using mortar joints. The load transfer in this case is primarily under compressive stress so that additional bending capacity through reinforcement does not need to be provided. If needed, other approaches combine reused steel profiles with concrete elements. Here, the profiles serve as the main load-bearing elements supporting RC slabs[17]. In contrast to the other approaches and although the major part of the load is transferred by the steel profiles, the concrete slabs contribute in bending, too.

For form finding of new structures made from reused modules, various optimization approaches have been derived mainly for the reuse of steel and timber components. These methods are based on, for example, Integer Linear Programming (ILP)[18], Evolutionary Algorithms (EA)[19], or extended algorithms of discrete truss optimization[20]. Often so-called ground structures that consist of a pattern of nodes connected by trusses serve as design domain. They define permitted module positions with corresponding lengths. The quantity and length of possible modules vary with the level of connectivity between the nodes that represent permitted module positions and corresponding lengths are used for the fundamental placement. On these, modules from a construction kit are binary placed, i.e. a position is assigned with a module or is not. Too large modules are either cut off or the ground structure is subsequently adapted with respect to the module lengths[21]. However, these modules are primarily subjected to axial loads so that the load-bearing capacity is ensured by stress restrictions[22,23]. Hybrid approaches that incorporate both reused and new modules can also be utilized with these methods. Compared to pure reuse, CO_2 emissions can be reduced[24].

Two essential things change when reusing almost arbitrary RC modules: Due to the varying geometry, i.e. module dimensions, the static system changes with respect to the placement of the modules and their joints. Moreover, the stiffness and load-bearing capacities within the system change due to the geometry of the modules' cross-sections, the reinforcement ratio and material strengths, too. Thus, the internal forces vary depending on the modules' placement. This results in a complex Combinatorial Optimization Problem (COP) already when considering simple systems or subsystems, such as frames or continuous beams, and becomes even more complicated with the size of the construction kit, i.e. the number of module types. Metaheuristics have proven to be particularly effective for COP[25,26], as has been shown, for example, for the permutation of concrete modules in modular structures consisting of only a few module types[27].

The paper aims at a method for designing new structures made from reused RC modules. Therefore, modules from a construction kit, which consists of different RC modules characterized by uncertain geometries and material parameters, form a structure using meta-heuristics. The objective is maximum utilization of the modules while maintaining geometrical boundary conditions and structural integrity. For this purpose, a construction kit is first generated and the associated load-bearing capacities of the modules are derived. Second, an agent-based preselection reduces possible combinations of the reused modules within the investigated system depending on geometric tolerance requirements. The reduced combinations form an Action List (AL) for the COP using metaheuristic with the objective of maximum utilization, thus generating an optimal placement of the existing RC modules for new structures.

2 | MATERIAL AND METHODS

2.1 | Problem statement - Reuse of RC elements for new structures

The form finding method is derived at the example of one-way floor slabs of high-rise buildings, since slabs as the simplest spatial structure usually form the basis of the architectural design. The slabs are supported by substructures and can for simplicity be designed separately from the rest of the structure as continuous beams subjected to bending and shear. The statical system to be investigated is a three-span beam with fixed supports. The construction kit comprises modules that adapt reused RC modules with inherent load-bearing capacities depending on their external and internal geometry and material parameters. It is assumed that modules from the deconstruction of a structure partially exhibit similar geometries and material properties and therefore can be consolidated to certain module types.

Depending on the position and stiffness of the modules and their connections, internal forces – for known loads – result. The placement strategy is controlled by both geometrical needs and the utilization of the modules' load-bearing capacity. Geometrically, the module combinations of the formed slab must not be too short, but also not exceed a tolerance range to avoid

unnecessary cut offs from the modules at the edges. Mechanically, the aim is to maximize utilization in order to reuse modules as efficiently as possible.

The placement strategy involves two steps: first, identifying all geometrically feasible module combinations, and then optimizing these combinations for maximum utilization using combinatorial optimization. The basic procedure is shown in Figure 1. After deconstruction (left), the existing RC modules, here slab elements, are grouped together in a construction kit consisting of different module types. Depending on the geometry and the material, they possess certain load-bearing capacities, in the form of M-N resistances (center) and bearable shear loads. Possible module type combinations are determined via the geometric tolerance requirements and yield the static system. Optimal combination and permutation ensures the load-bearing capacity and also maximizes the utilization (right).

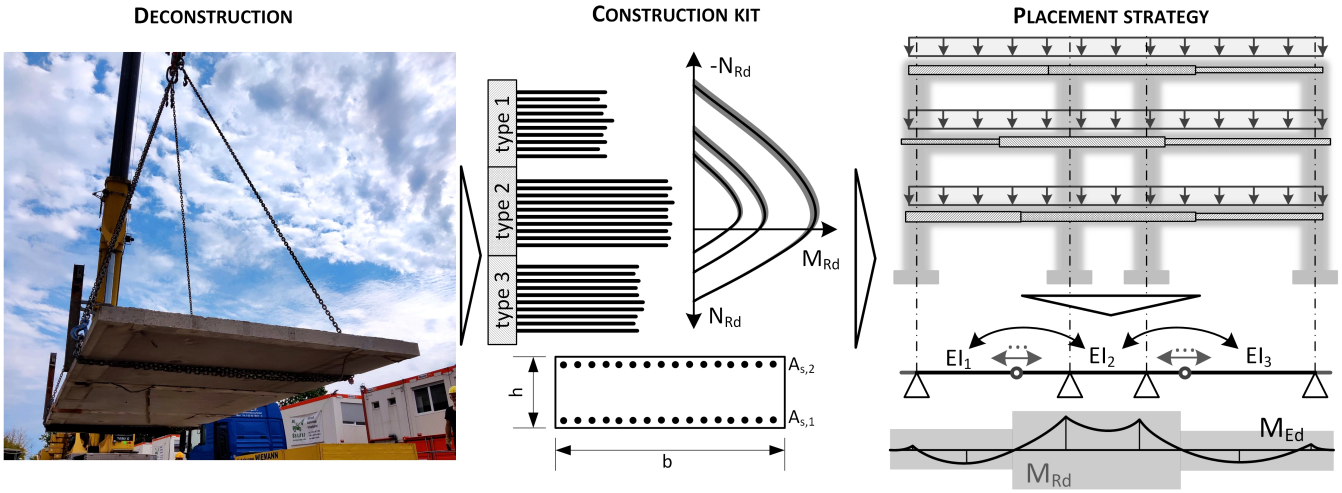

FIGURE 1 Method for the reuse of structural RC modules: The dismantled modules from deconstruction are consolidated to construction kits with respect to their geometry and load-bearing capacity and finally reused in new structures steered by a geometrical and mechanical placement strategy

2.2 | Construction kit of reused elements

2.2.1 | Sampling of geometry and material properties

Lacking a real use case is compensated for by artificial generation of a construction kit. The RC modules therein are generated using Monte Carlo sampling of the geometrical and mechanical parameters. The modules consist of normal-strength concrete with symmetrical steel reinforcement ($A_{s1} = A_{s2}$) and exhibit the common reference width of $b = b_w = 1$ m for slabs. From this data, load-bearing capacities can be derived to simulate a construction kit of reused modules. In general, distinction is made between five module types, which differ in geometry i.e. length l, height h, reinforcement distances to the surface $d_{1,2}$ and amounts $A_{s1,2}$ as well as material properties, i.e. characteristic concrete compressive f_{ck} and reinforcement yield strengths f_{yk}, and regarding their scatter (Table 1). For each module type and its associated uncertainties, 20 modules are sampled so that in total 100 modules form the construction kit.

Typically, dimensions and mechanical parameters exhibit variation, which is, in a probabilistic approach, considered by associated distribution functions. The distribution function of the length l is uniform $\mathcal{U}$ with type-specific tolerance limits t. Hereby, t defines the absolute limits from the mean μ. The height h and the distances to the reinforcement d_1 and d_2 are normally distributed $\mathcal{N}$. The mean height of the modules varies from 16 to 28 cm and the mean distances $d_{1,2}$ between 3 and 5 cm. The variation of these geometric parameters is described by the standard deviation σ. It is based on a tolerance t, which captures the

TABLE 1 Stochastic properties of the five module types in the construction kit.

		l [m]			h [cm]			$A_{s1,2}$ [cm^2]	$d_{1,2}$ [cm]			f_{yk} [N/mm^2]	f_{ck} [N/mm^2]		
	amount	μ	t	pdf	μ	σ	pdf	μ	μ	σ	pdf	μ	μ	σ	pdf
type 1	20	4.5	±0.2	$\mathcal{U}$	20	0.5	$\mathcal{N}$	3.77[a]	4	0.25	$\mathcal{N}$	500[a]	30	3	$\mathcal{LN}$
type 2	20	5.5	±0.3	$\mathcal{U}$	24	0.5	$\mathcal{N}$	5.13[a]	4	0.25	$\mathcal{N}$	500[a]	40	3	$\mathcal{LN}$
type 3	20	6.7	±0.5	$\mathcal{U}$	28	0.5	$\mathcal{N}$	7.54[a]	5	0.25	$\mathcal{N}$	500[a]	55	3	$\mathcal{LN}$
type 4	20	3	±0.3	$\mathcal{U}$	16	0.5	$\mathcal{N}$	1.88[a]	3	0.25	$\mathcal{N}$	500[a]	30	3	$\mathcal{LN}$
type 5	20	3.8	±0.25	$\mathcal{U}$	18	0.5	$\mathcal{N}$	2.57[a]	3	0.25	$\mathcal{N}$	500[a]	40	3	$\mathcal{LN}$

$\mathcal{U}$ - uniform; $\mathcal{N}$ - normal, $\mathcal{LN}$ - log-normal
[a]constant

confidence interval as a function of the probability value z_p, usually set to 2 for RC components[28]. As the tolerance of h is set to 1 cm, and that of d_1 and d_2 to 0.5 cm, the standard deviations in Table 1 are obtained from Equation 1.

$$\sigma = \frac{t}{z_p} \tag{1}$$

Usually, existing components are originally made of normal-strength concrete. But, the compressive strength f_{ck} has increased with time. As a resistance quantity its variation is described with a log-normal distribution $\mathcal{LN}$. A standard deviation of 3 N/mm^2 indicates good concrete quality. In comparison to the uncertain parameters, the steel strength of $f_{yk} = 500$ N/mm^2 and the reinforcement amounts ($A_{s1} = A_{s2}$) are assumed to be deterministic to account for precise production. The reinforcement amounts reflect typical mesh reinforcement of the building practice. Besides the general placement, the resistance and thus the takeable forces of the modules depend on their (bending) stiffness. While the moment of inertia I results from the geometry, the Young's modulus is a material property. In accordance with DIN EN 1992-1-1 the mean elastic modulus of the concrete E_{cm} is determined with Equation 2 as a function of the mean concrete strength f_{cm}.

$$E_{cm} = 22{,}000 \cdot \left(\frac{f_{cm}}{10}\right)^{0.3} \tag{2}$$

$$\text{with:} \quad f_{cm} = f_{ck} + 8$$

2.2.2 | Load-bearing capacity

The 100 modules of the construction kit are fully specified with the values provided in Section 2.2.1 and the associated variations in Table 1. Assuming constant conditions over the entire module length, this also applies to the load-bearing capacities (M_{Rd}, N_{Rd} and V_{Rd}). As common with DIN EN 1992-1-1[29], these are calculated separately for bending with longitudinal forces and shear. For slabs, the latter is usually done with the approach for members without reinforcement. For convenience, these resistances and the associated input variables are documented in Appendix A.

2.2.2.1 | *Bending design*

Since all modules possess rectangular cross-sections and symmetrical reinforcement (Figure 2, left) their bending capacity can be obtained from classical M-N design charts[30] (cf. Figure 2, right) observing the limit strains of normal-strength concrete and reinforcement steel type B500[29]. The stress-strain relationship for normal-strength concrete follows the parabolic rectangular diagram and delivers the design strength f_{cd}.

$$f_{cd} = \alpha_{cc} \frac{f_{ck}}{\gamma_c} \tag{3}$$

$$\text{with:} \quad \alpha_{cc} = 0.85$$
$$\gamma_c = 1.5$$

The material law of the reinforcement is bi-linear with a horizontal branch at the design yield strength f_{yd} (Equation 4). The Young's modulus of the linear-elastic branch is E_s = 200,000 MPa.

$$f_{yd} = \frac{f_{yk}}{\gamma_s} = 435 \text{ N/mm}^2 \tag{4}$$

$$\text{with:} \quad \gamma_s = 1.15$$

With two strains, e.g. the maximum concrete strain at the compressed edge ε_{c2} and the steel strain in the lower reinforcement layer ε_{s1}, the strain distribution in the cross-section is uniquely defined (Figure 2, left). x denotes the proportion of height in compression. Moreover, with the two material laws, the transition from the strain space to the design stress space is possible any time. The stresses and their associated effective areas (A_{s1}, A_{s2} and $A_c = x \cdot b$) provide the forces (F_{s1d}, F_{s2d} and F_{cd}) that yield the design resistances (N_{Rd} and M_{Rd}) via the equilibrium conditions.

$$N_{Rd} = F_{s1d} - F_{s2d} - F_{cd} \tag{5}$$

$$M_{Rd} = F_{s1d} \cdot (\frac{h}{2} - d_1) + F_{s2d} \cdot (\frac{h}{2} - d_2) + F_{cd} \cdot (\frac{h}{2} - a) \tag{6}$$

with: F_{sid} - force in the reinforcement layer A_{si}
F_{cd} - compressive force in the concrete
a - distance from top to the concrete force

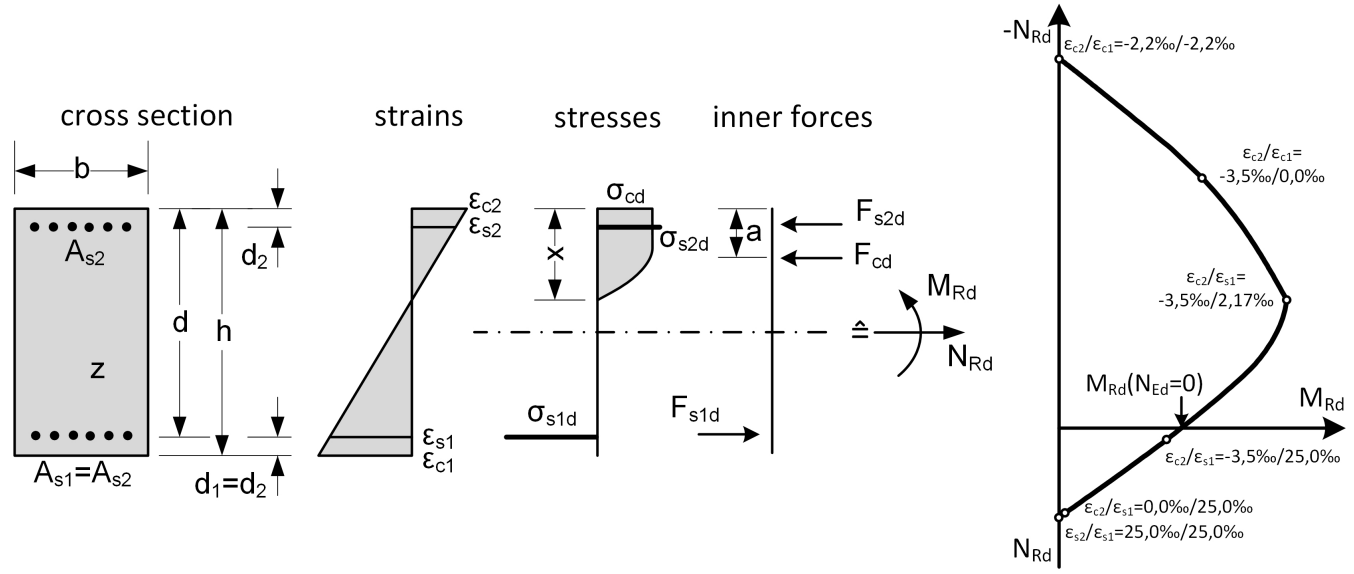

FIGURE 2 Dimensions, strain and stress distributions, and inner forces along with resulting M-N design chart for a rectangular RC cross section

Computation for all admissible strain combinations specifies a resistance curve that covers all bearable M-N-ratios for each RC module with respect to geometry and reinforcement layout. In Figure 2 (right) a general diagram is shown in which characteristic strain states are highlighted. This diagram uniquely assigns a bending resistance M_{Rd} to each axial force N_{Ed}. However, due to the statical system of slabs investigated here, subjected to vertical forces only, M_{Rd} is always read from the diagram for $N_{Ed} = 0$, i.e. for pure bending.

2.2.2.2 | *Shear design*

The shear resistance of members without shear reinforcement and axial loads ($\sigma_{cp} = N_{Ed}/A_c = 0$) is calculated from Equation 7[29]:

$$V_{Rd} = \left[\frac{0.15}{\gamma_c} \cdot k \cdot (100\rho_l f_{ck})^{1/3}\right] \cdot b_w d \tag{7}$$

with:
$$\gamma_c = 1.5$$
$$k = 1 + \sqrt{\frac{200}{d\ [\text{mm}]}} \leq 2$$
$$b_w = 1\ \text{m}$$
$$d = h - d_1$$
$$\rho_l = \frac{A_{s1}}{b_w \cdot d} \leq 0.02$$

It depends on the geometry and the concrete strength. k is a scaling factor, d denotes the statical height and ρ_l the reinforcement ratio. In general, a minimum value $V_{Rd,min}$ must be considered for the shear resistance V_{Rd} according to Equation 7. However, this only applies to low reinforcement ratios, which are not encountered in the reused modules.

2.3 | System and Assembly

The statical system is specified as a three-span beam with outer span lengths of 4.5 m and an inner span length of 3 m (Figure 3). In addition to the dead load g_k of the modules, the system is subjected to a variable line load of $q_k = 2$ kN/m, which corresponds to service loads in conventional building construction. g_k depends on the individual cross-section of the module and the weight of concrete $\gamma_c = 25\,\text{kN/m}^3$. All combinations must have 3 modules to ensure a static determinate system. A surplus is tolerated but limited to $\triangle = 1$ m on each side. Their arrangement on the supports always ensures that it is the same on both sides. This enables a certain variability of the modules and at the same time avoids excessive overlength that could impair neighboring buildings. By contrast, too short combinations are (statically) not feasible. For design, the connections of the modules are mechanically modeled as ideal moment joints so that only shear and axial forces are transmitted between the modules. After placing, the internal forces are calculated and compared locally to the modules' load-bearing capacities to cover the global load-bearing capacity of the system. Comparison considers the ultimate limit state with design values for actions and resistances according to the partial safety concept.

As said, the created construction kit consists of $n = 100$ modules. $k = 3$ of these are put together to form a load-bearing structure. Mathematically, the number of possible permutations P_{MC} is determined by the laws of combinatorics according to Equation 8, whereby order matters and no repetitions are permissible. It yields the vast number of 970,200 module combinations. Clearly, the computational effort of numerical modelling that many combinations is too expensive. Therefore, it is advisable to first reduce it by preselecting only the geometrically feasible ones. For simplicity this is done with agent-based modeling on the basis of the five module types introduced above (Section 2.4). In general, interval analysis is also suitable for the same task[31].

$$P_{MC}(n,k) = \frac{n!}{(n-k)!} \tag{8}$$

Just the remaining combinations are numerically modelled by guidance of metaheuristics, which specifically check their load-bearing capacities. Since the latter is explicitly done on the level of modules and not on types, again geometrically unfeasible solutions might occur that are rejected within in the metaheuristics (Section 2.5).

2.4 | Geometric Preselection of Structural Elements using Agent-Based Modeling

While many traditional optimization algorithms, such as Genetic Algorithms (GAs)[32], the Greedy Search Algorithm[33], or the Hungarian Algorithm[34], have been proven powerful in solving complex combinatorial problems, an Agent-based Modeling

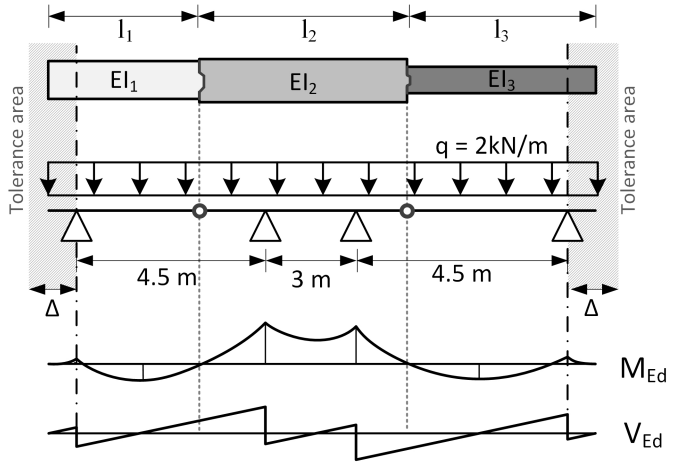

FIGURE 3 Statical system with dimensions and loads for an exemplary positioning of modules with qualitative moment and shear force

(ABM) approach for the geometric preselection of elements was chosen here. The preselection problem is particularly challenging because it involves dynamically exploring a vast array of potential configurations to filter out unsuitable combinations early in the process. Unlike final selection, which focuses on optimizing within a narrowed set of options, preselection must handle high variability and complexity from the outset.

ABM is especially suited for this task due to its ability to simulate numerous agents exploring different combinations simultaneously, thus efficiently navigating and narrowing down the extensive solution space. Its flexibility and adaptability makes it suited for handling the dynamic and iterative aspects of solving complex geometric problems, where multiple variables and evolving criteria must be continuously balanced[35]. The challenges originate from the continuous evaluation and adjustment of module combinations as new geometric constraints are introduced or existing ones are modified. ABM allows agents to independently test and modify combinations of modules, responding to changes in requirements and optimizing configurations in real-time.

Moreover, ABM presents a robust alternative to other optimization methods by simulating decentralized decision-making processes that can adapt and evolve through local interactions and simple behavioral rules, fostering the exploration of the wide solution spaces that characterize early design stages in construction[36]. Behavioral rules are the basic guidelines that dictate how agents make decisions and interact with their environment and other agents. Here, they include selecting random combinations of modules, evaluating their total length against the target, and modifying combinations based on mutation rates. Decentralized decision-making in ABM characterizes that multiple agents make their decisions independently based on local information and interactions rather than relying on a single centralized control entity. This decentralized approach allows for flexibility and adaptability, as agents can explore different parts of the solution space simultaneously.

The implemented ABM simulates a population of agents, each representing a decision-making entity in preselecting suitable combinations of three modules from the given set of module types. Figure 4 illustrates the ABM for the geometric preselection, evaluation, and optimization of module type selection, and depicts the model's main constituents, namely "GirderModel" and "GirderAgent", along with the sequence of actions from initialization to compiling results. Each agent starts with a random combination of modules and iterates through a process of selection and mutation, akin to a simplified form of genetic crossover and mutation seen in GA. However, unlike GAs where the crossover and mutation are centrally controlled and applied, in the model presented, each agent autonomously adapts its strategy based on localized performance metrics. This autonomy can prevent premature convergence on suboptimal solutions by preserving a diverse set of potential solutions throughout the simulation run.

Each module type covers the geometric characteristics, e. g. lengths according to Table 1, of its members. In total P_{MTC} possibilities exists to combine $k = 3$ out of $n = 5$ module types. For the construction set specified, the total number of module type combinations $P_{MTC} = 125$ is obtained from Equation 9, mathematically by permutation with repetition and when order matters.

$$P_{MTC}\,(n, k) = n^k \tag{9}$$

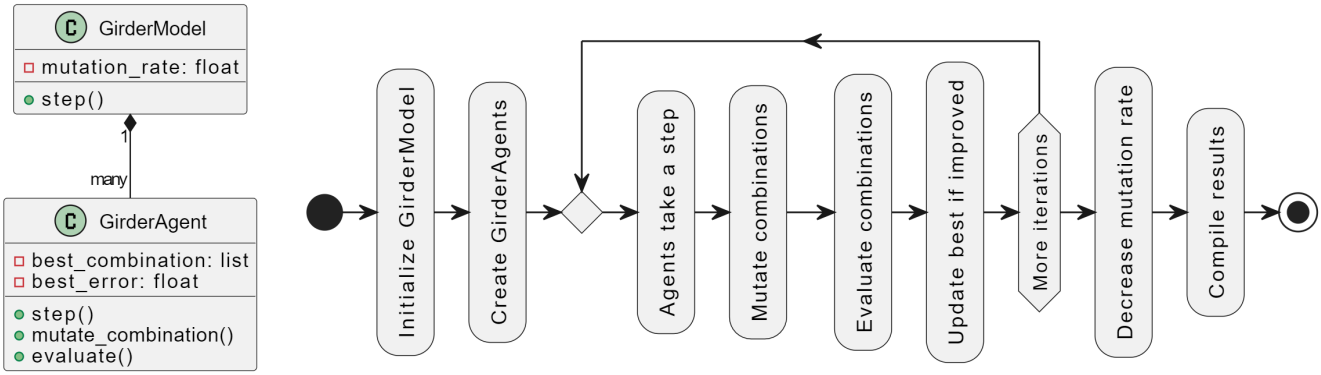

FIGURE 4 ABM for geometric preselection, evaluation, and optimization of type selection. Model constituents (left) and actions (right).

Length-matching solutions that consist of only two modules are intentionally neglected due to the potential of these longer modules to be more effectively utilized in applications requiring wider spans. Since there could potentially be module types of exactly the same dimensions, it is also noted that these may be used multiple times within a single configuration.

The key criteria for selecting suitable modules from the given set of module types shown in Figure 5 (left) is the difference of the length resulting from the combination of three chosen modules to the spanning distance of the given support locations. A minimum resulting length of 12 meters is required, module combinations that span further are considered viable, but less desirable. Combinations that result in a span shorter than 12 meters are considered non viable and therefore removed from the list of viable solutions.

Agents assess the effectiveness of their module combinations against the target span length. Combinations that do not meet the minimum required length are discarded immediately, while those that exceed the target length are subjected to a penalty proportional to their surplus. In the model, each agent calculates an error as the absolute difference between the total length of a combination and the target span length, effectively quantifying the material surplus. This error serves as a penalty, directing the agents toward the most material-efficient combinations. Only those combinations where the calculated error is less than the agent's previously recorded best error are considered improvements and are retained for further evaluation. Consequently, agents refine their search iteratively, always seeking to minimize this error, thereby reducing excess material use. Through this mechanism, the model promotes an optimized search for module combinations that meet or slightly exceed the target length, enhancing material efficiency in structural design.

The ABM prioritizes the discovery of diverse, near-optimal solutions rather than converging on a single global optimum. This approach is particularly advantageous in architectural preselection, where multiple viable solutions offer the flexibility to adapt to changing design requirements or material availability.

In the presented model convergence plot (Figure 5, right), an initial wide distribution of total module lengths, reflecting extensive exploratory behavior by the agents, is observed . With successive iterations, there is a discernible increase in the frequency of solutions meeting or exceeding the target length of 12 meters, as evidenced by the growing density of blue points around the horizontal red line indicating the optimal length of 12 meters resulting from a module combination, which suggests progressive learning within the agent population. In the presented model, a total of 10 agents are used to select, calculate, and evaluate module combinations. To share the best-fitting findings among the agents, the GirderModel class continuously updates and tracks the best combination found by any agent, allowing other agents to adopt this global best solution. Red points below the target length occur mainly within the first half of the simulation, indicating early exploration and a potential presence of local optima.

The convergence pattern observed underscores the model's capability to balance exploration with the exploitation of viable solutions over successive iterations. The resulting possible combinations provide the basis for a load-bearing capacity-based placement using metaheuristics (Section 2.5).

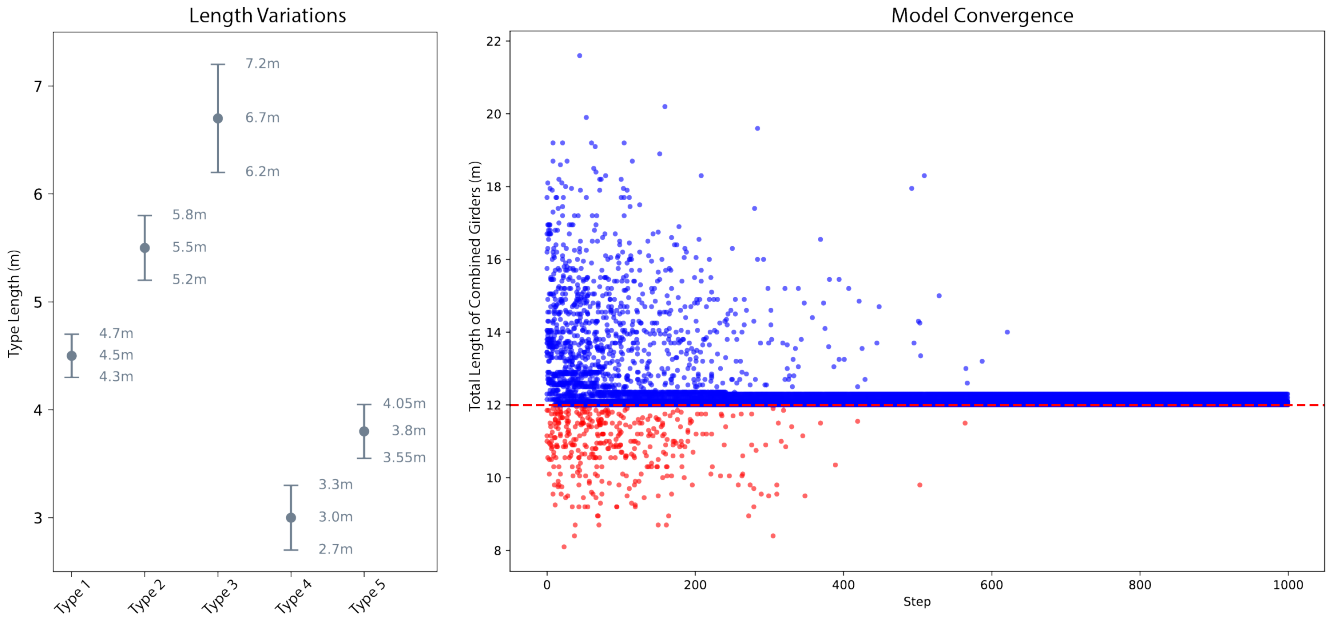

FIGURE 5 Overview of module types and converging module selection over time.

2.5 | Metaheuristics

2.5.1 | Basics

For Combinatorial Optimization Problems (COPs) the goal is to find an optimal combination of design variables from a finite set of values. Consequently, the number of possible solutions grows with the number of variables, respectively with the size of the finite set. Thus, COPs can be hard to solve in reasonable computational time. Dealing with a large number of possible solutions and lacking on problem-specific knowledge, such as gradient information of the objective function, highlights where metaheuristics can express their potential. Combining local search algorithms with methods to overcome local minima, they provide a method to find either the global optimum or to approximate it by "trial and error" and without evaluating the complete solution space[37]. Furthermore, due to their generality, existing methods can be adapted to various kinds of optimization problems. Key is to define an objective function related to a suitable solution and the neighborhood of this solution[38].

Metaheuristics are mainly categorized into trajectory-based and population-based algorithms[39,37]. Trajectory-based algorithms incrementally build a path through the solution space. Based on criteria of exploration and exploitation, at each step a single neighboring solution is chosen to extend the trajectory. Thereby, without getting stuck, local neighborhoods can be searched thoroughly to find a better solution. In contrast, population-based algorithms handle multiple solutions at one step which results in a more diverse investigation of the solution space. Nevertheless, this often requires more computational resources at a time.

Therefore, the COP of placing reused RC modules is tackled with well established methods of trajectory-based algorithms, namely Simulated Annealing (SA) and Tabu Search (TS), which have been shown to perform well for a similar COP[27].

2.5.2 | Formulation of the Optimization Problem

Based on the problem stated in section 2.3, the goal is to combine a structure from three modules, mounted on four supports. For this purpose, a construction kit of 100 modules from 5 module types is sampled (cf. Appendix A). The aim is to find an optimal placement of three out of 100 sampled modules.

A placement of modules is represented by the solution vector $\boldsymbol{S}$. The length of $\boldsymbol{S}$ is restricted to $N = 3$ individual modules S_1, S_2, and S_3 from the sampled kit:

$$\boldsymbol{S} = [S_1, S_2, S_3] \tag{10}$$

The quality of a solution $\boldsymbol{S}$ is measured by the objective function $f(\boldsymbol{S})$ which describes a minimization problem. Aiming for maximum bending utilization, $f(\boldsymbol{S})$ is reformulated to the difference between 1 and the mean of the three modules maximum bending moment utilization factors η_{M,S_m} (Eq. 11). Small objective function values correspond to larger mean utilization factors and vice versa. For each module S_m, it is ensured that the maximum bending moment M_{max,S_m} or the maximum shear force V_{max,S_m} does not exceed the associated capacities M_{Rd,S_m} or V_{Rd,S_m}. These restrictions are implemented by means of inequality constrains via Eqs. 12 and 13. The internal moments and forces are evaluated using parametric finite element modelling in the parametric design language "ANSYS Mechanical APDL".

$$\min \quad f(\boldsymbol{S}) = 1 - \left(\frac{1}{N} \sum_{m=1}^{N} \eta_{M,S_m} \right) \tag{11}$$

$$\text{s.t.:} \quad \eta_{M,S_m} = \frac{\left| M_{max,S_m} \right|}{M_{Rd,S_m}} \leq 1 \tag{12}$$

$$\eta_{V,S_m} = \frac{\left| V_{max,S_m} \right|}{V_{Rd,S_m}} \leq 1 \tag{13}$$

$$\text{with:} \quad m \in [1, 2, 3]$$

Defining a neighborhood structure is essential for constructing efficient metaheuristic search procedures. Starting from a solution $\boldsymbol{S}_i$, a neighboring solution $\boldsymbol{S}_j$ is generated using one of two kinds of Action Type (AT):

1. Replace an entry of $\boldsymbol{S}_i$ with another arbitrary module from the sampled construction kit (AT1),
2. Swap two entries within $\boldsymbol{S}_i$ (AT2).

Thereby, an Action List (AL) is formed that contains all possible actions of AT1 (replacements) and AT2 (swapping) which can generate all possible neighborhoods of module combinations. In the use case with 100 modules in the construction kit, the AL comprises 302 entries. 300 are accounted for by AT1 and 2 by AT2, since each configuration consists of three modules. Excluding symmetry, there are 3 options to arrange the three modules of a configuration. For AT2, 2 relevant swaps remain: first and second position, or second and third position. The remaining one is again irrelevant for reasons of symmetry. Symmetry exists here in particular due to the specific arrangement of supports and an always equal surplus on both sides. In addition, the AL is restricted to the combinations of the feasible geometric preselection obtained in section 2.4. Practically, for each module type combination of the preselected combinations a specific AL is defined incorporating the specific modules of the chosen types. Both algorithms SA and TS are using this AL as reduced solution space.

2.5.3 | Simulated Annealing

The local search algorithm SA [40], inspired by physics, works analogous to temperature cooling processes of solids. Particles of a melted solid behave randomly. If the solid is cooled down gradually and slow enough, the particles order in their ground state where they form a lattice structure. The energy of the solid's ground state is minimal [38]. Transferring this concept to the metaheuristic search algorithm, the energy E is interpreted as the objective function value $f(\boldsymbol{S}_i)$, whereby $\boldsymbol{S}_i$ represents a certain state of the solid. When a neighboring solution is generated and its evaluated energy $f(\boldsymbol{S}_j)$ is smaller than the previous one $f(\boldsymbol{S}_i)$, the neighbor solution $\boldsymbol{S}_j$ is accepted as new current solution $\boldsymbol{S}_i$. Subsequently, new neighboring solutions are generated, transitioning from the current solution $\boldsymbol{S}_i$. In the alternative case with $f(\boldsymbol{S}_j) > f(\boldsymbol{S}_i)$, SA makes use of the Metropolis criterion [41] (Eq. 14). If it holds true, it effects the acceptance of a worse solution as the current solution. This concept of building the search

trajectory facilitates overcoming local minima while searching the solution space.

$$r < e^{\frac{\Delta E}{T}} \tag{14}$$

$$\text{with:} \quad r = rand[0,1]$$
$$\Delta E = f(\boldsymbol{S}_i) - f(\boldsymbol{S}_j)$$

The Metropolis criterion checks whether a random number r between zero and one is smaller than an exponential term dependent on the energy difference ΔE and a current temperature T. The temperature parameter T controls the algorithm's cooling process and is gradually reduced by factor α_T until it reaches an end temperature T_{end}. If the cooling schedule is slow enough, the algorithm converges to the global minimum. α_T is typically chosen between 0.7 and 0.99 for a so called geometric cooling schedule[37]:

$$T := \alpha_T \cdot T \tag{15}$$

At each cooling step characterized by a current temperature T, n_{sub} neighbor solutions are evaluated. Higher temperatures effect higher acceptance probabilities of these solutions. Thus, at the beginning of the search procedure the solution space is explored more widely. Lower temperatures lower the acceptance probability and the search trajectory exploits regions where the objective function value is closer to the global minimum. If the Metropolis criterion holds true (see Eq. 14), ΔE must be negative. Hence, larger absolute values of ΔE correspond with lower acceptance probabilities while lower absolute values of ΔE correspond with higher acceptance probabilities.

The implemented SA algorithm is illustrated in the iteration scheme in Fig. 6. It is initialized with a random, yet feasible solution $\boldsymbol{S}_0$ as the best-known solution $\boldsymbol{S}^*$ that is updated throughout the algorithm's evaluations. Moves to build the search trajectory are randomly picked from the specific AL. Thereby, the code prevents the same move from being applied twice to the same solution. When the SA algorithm terminates by reaching temperature T_{end}, the approximate global minimum, respectively the true minimum is the last found solution $\boldsymbol{S}^*$. The relevant parameters for the stated optimization problem are found heuristically and summarized in Tab. 2. T_{start} is scaled to the domain of $f(\boldsymbol{S})$ between zero and one. T_{end} as well as α_T are chosen such that the cooling schedule is slow and long enough, whilst ensuring that the algorithm terminates in a given timespan. Selecting n_{sub} with around 10 percent of the ALs size is reasoned in a trade-off between computational time and sufficient exploitation at a temperature step.

TABLE 2 Chosen parameters for the implemented SA algorithm.

initial temperature [K]	end temperature [K]	cooling rate [-]	subiterations [-]
T_{start}	T_{end}	α_T	n_{sub}
0.5	10^{-3}	0.95	30

2.5.4 | Tabu Search

The TS[42] represents a local search procedure with the possibility of escaping local minima similar to SA. In contrast, the TS generates a memory structure which prevents the algorithm to loop back to previous solutions[39]. TS builds its search trajectory based on constructing n_N neighborhoods $N(\boldsymbol{S}_i)$ for a start solution $\boldsymbol{S}_i$. The amount of examined neighboring solutions within $N(\boldsymbol{S}_i)$ is fixed by the number n_{sub}. While a larger n_N goes along with more exploration, increasing n_{sub} effects more exploitation.

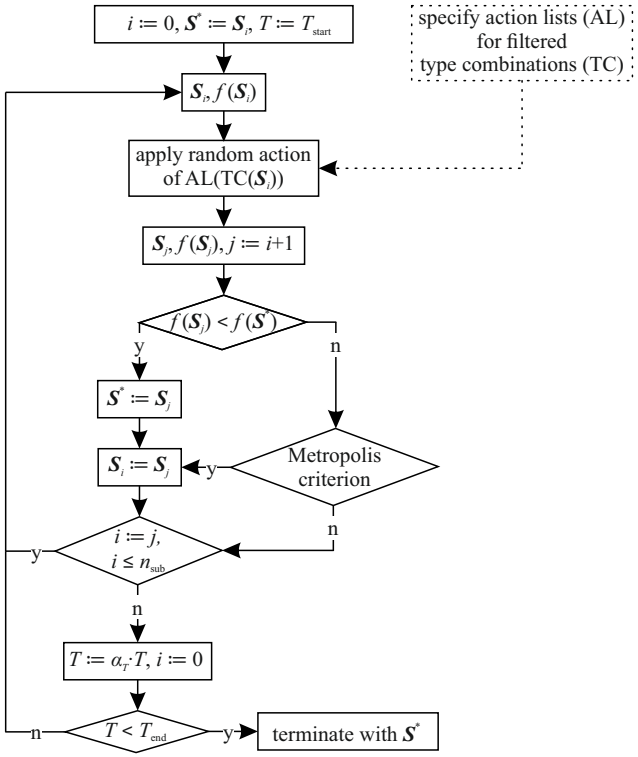

FIGURE 6 Iteration scheme for implemented SA algorithm.

After generating a full neighborhood the best solution $\boldsymbol{S}_j$ is chosen from $N(\boldsymbol{S}_i)$ to be the new start solution $\boldsymbol{S}_i$:

$$\boldsymbol{S}_j := \underset{\boldsymbol{S} \in \boldsymbol{N}(\boldsymbol{S}_i)}{\operatorname{argmin}} \quad f(\boldsymbol{S}) \tag{16}$$

At this point, the concept of a memory structure organized as Tabu List (TL) determines the acceptance of $\boldsymbol{S}_j$. Accepted solutions $\boldsymbol{S}_j$ of previously investigated neighborhoods have a distinct Action Index (AI) that has led to their generation. This AI is associated to a value on the TL which, if non-zero, blocks the acceptance of solution $\boldsymbol{S}_j$ as new start solution $\boldsymbol{S}_i$. Furthermore, the value specifies the amount of upcoming neighborhoods, where solutions generated by the associated AI are tabu. Firstly, it is set to a predefined Tabu Duration (TD). Subsequently, for each upcoming neighborhood $N(\boldsymbol{S}_i)$, the value of TD is reduced by one until it becomes zero. Thus, $\boldsymbol{S}_j$ is chosen to be the best solution from $N(\boldsymbol{S}_i)$, provided that the AI that led to its generation is associated with a TD of zero. If Eq. 16 is enhanced by this condition, Eq. 17 results. It can only be ignored if an aspiration criterion[43] is met. This criterion becomes active if $\boldsymbol{S}_j$ is the global best-known solution $\boldsymbol{S}^*$, then $\boldsymbol{S}_j$ is accepted as $\boldsymbol{S}_i$ in any case.

$$\boldsymbol{S}_j := \underset{\boldsymbol{S} \in \boldsymbol{N}(\boldsymbol{S}_i), TD(AI(\boldsymbol{S}))=0}{\operatorname{argmin}} \quad f(\boldsymbol{S}) \tag{17}$$

Figure 7 illustrates the implemented TS in detail. Since TS is restricted to n_N neighborhoods it may lag on exploration of the solution space. Therfore, a diversification strategy[43] is introduced. One part of diversification is to implement a global stagnation criterion. If $\boldsymbol{S}^*$ is not improving for a fixed number of investigated neighborhoods (so-called diversification limit) the new start solution $\boldsymbol{S}_i$ becomes a random feasible solution. This allows other regions of the solution space to be explored. Another part of diversification is that in contrast to the SA algorithm not only random actions are applied to generate neighboring solutions. While for the SA it is randomly possible that e.g. only AT1 is applied, rather all actions of AT2 are ensured to be used for constructing $N(\boldsymbol{S}_i)$ in the TS. Analogous to SA, the parameters in Table 3 are found heuristically and adapted to the specific problem.

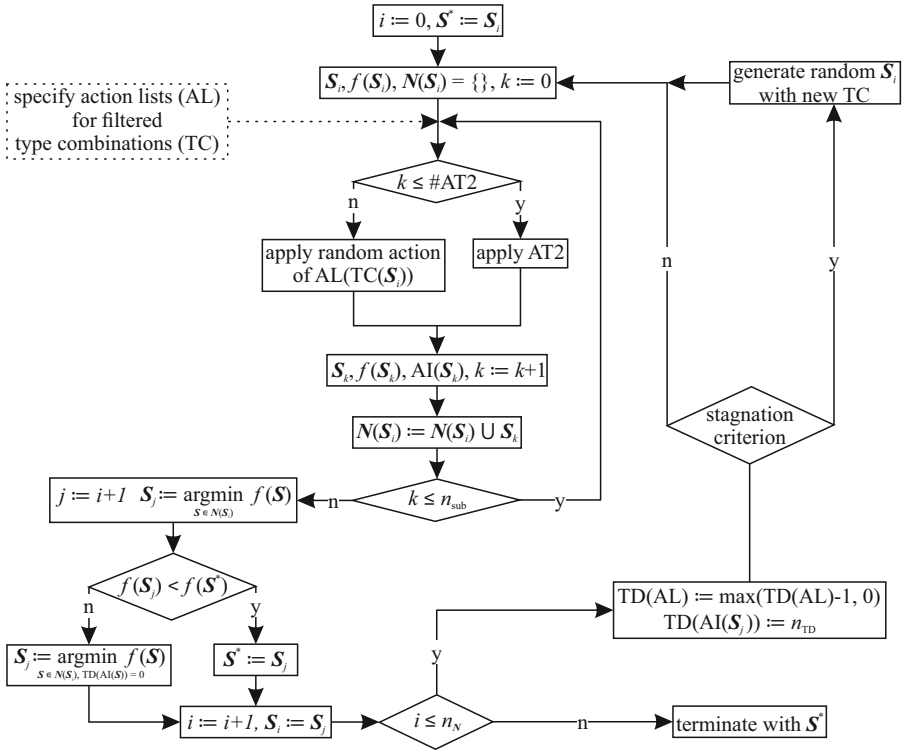

FIGURE 7 Iteration scheme for implemented TS algorithm.

TABLE 3 Chosen parameters for the implemented TS algorithm.

investigated neighborhoods [-]	neighborhood size [-]	tabu duration [-]	diversification limit [-]
n_N	n_{sub}	TD	DL
49	75	10	10

3 | RESULTS

3.1 | Preselection of geometrically feasible combinations

Figure 8 shows those 18 module type combinations that achieve the minimum target length of 12 m with three modules and at the same time comply with the total length of 14 m at maximum (a maximum surplus of 1 m per side for a set of three modules is tolerated). This set was identified during preselection with Agent-based Modeling (ABM) (cf. Section 2.4). The visualisation employs histograms that were generated with the minimum, maximum and mean module lengths of each type from Table 1 for convenience. The width of the histograms indicates that certain module type combinations offer a higher degree of length flexibility than others. Some fall completely within the permissible range, others merely touch it.

Among the feasible 18 combinations are 6 with three different, 2 with three identical and 10 with two identical module types. If the order in a combination is also taken into account via the associated case-specific numbers of possible permutations according to Equation 18, the total number increases to $68 = 6 \cdot 6 + 2 \cdot 1 + 10 \cdot 3$ (ordered combinations or permutations).

$$\begin{aligned} &\text{3 different:} \quad 6 = \binom{3}{1}\binom{2}{1}\binom{1}{1} = 3 \cdot 2 \cdot 1 = 3! \\ &\text{3 identical:} \quad 1 = \binom{1}{1} = \binom{3}{3} = 1! \\ &\text{2 identical:} \quad 3 = \binom{3}{2} = \frac{3!}{(3-2)! \cdot 2!} \end{aligned} \tag{18}$$

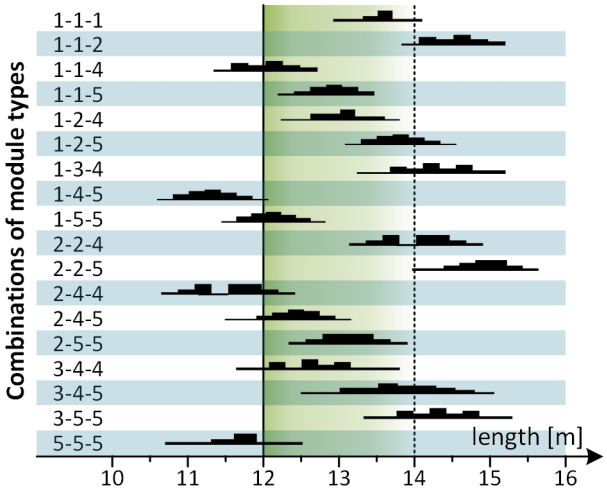

FIGURE 8 Feasible combinations of module types in the acceptable range (green area)

If the associated options for picking modules from the 5 types according to Equation 19 are considered, too, the transition from the type level to the module level can be performed. Just there, the efficiency of preselection can be evaluated through quotas.

$$\begin{aligned}
&\text{3 different:} \quad 10 = \binom{5}{3} = \frac{5!}{(5-3)! \cdot 3!} \\
&\text{3 identical:} \quad 5 = \binom{5}{1} = \frac{5!}{(5-1)! \cdot 1!} \\
&\text{2 identical:} \quad 20 = \binom{5}{1}\binom{4}{1} = \frac{5!}{(5-1)! \cdot 1!} \cdot \frac{4!}{(4-1)! \cdot 1!} \quad \text{or} \quad \frac{5!}{(5-2)!}
\end{aligned} \tag{19}$$

According to the laws of combinatorics, among the total number of module type permutations from Equation 9 $P_{MTC} = 125 = 5 \cdot 1 + 20 \cdot 3 + 10 \cdot 6$ are 5 with three identical, 60 with three different and another 60 with two identical module types. With this split, both P_{MTC} and the by preselection reduced number of combinations can be transferred to the module level, taking into account the likewise case-specific associated options of picking 3 modules from 20 according to Equation 20.

$$\begin{aligned}
&\text{3 different:} \quad \binom{20}{1} \cdot 1! \cdot \binom{20}{1} \cdot 1! \cdot \binom{20}{1} \cdot 1! = 20 \cdot 20 \cdot 20 = 8000 \\
&\text{3 identical:} \quad \binom{20}{3} \cdot 3! = \frac{20!}{(20-3)! \cdot 3!} \cdot 3! = 20 \cdot 19 \cdot 18 = 6840 \\
&\text{2 identical:} \quad \binom{20}{2} \cdot 2! \cdot \binom{20}{1} \cdot 1! = \frac{20!}{(20-2)! \cdot 2!} \cdot 2! \cdot \frac{20!}{(20-1)! \cdot 1!} \cdot 1! = 20 \cdot 19 \cdot 20 = 7600
\end{aligned} \tag{20}$$

Thus, P_{MC} from Equation 8 is drastically reduced from initially 970, 200 to $529,680 = 6 \cdot 6 \cdot 8000 + 2 \cdot 1 \cdot 6840 + 10 \cdot 3 \cdot 7600$ remaining combinations, which form the solution space for the metaheuristics. This indicates the efficacy of preselection using the Agent-based Modeling (ABM) method, which allows around 45% of all permutations to be excluded from further consideration. By the way, the efficacy should not be assessed from the remaining fraction of type combinations P_{MCT} ($68/125 \approx 0,54$) which is here by chance numerically similar to the module one but generally neglects the true frequencies of the three portions of the split.

Figure 9 shows the resulting length of remaining combinations for individual modules. The graph depicting the top 100 module combinations by total length illustrates the efficacy of the ABM in converging towards the target span of 12 meters. It reveals a notable clustering of combination lengths around the target, with a gradual increase in the surplus material, indicating a nuanced exploration of the solution space. The diversity of solutions found confirms the model's ability to adapt and find multiple viable options, essential for accommodating varying design requirements and material constraints. The close grouping of many combinations near the minimum length suggests that the most successful combinations within the given set of girder

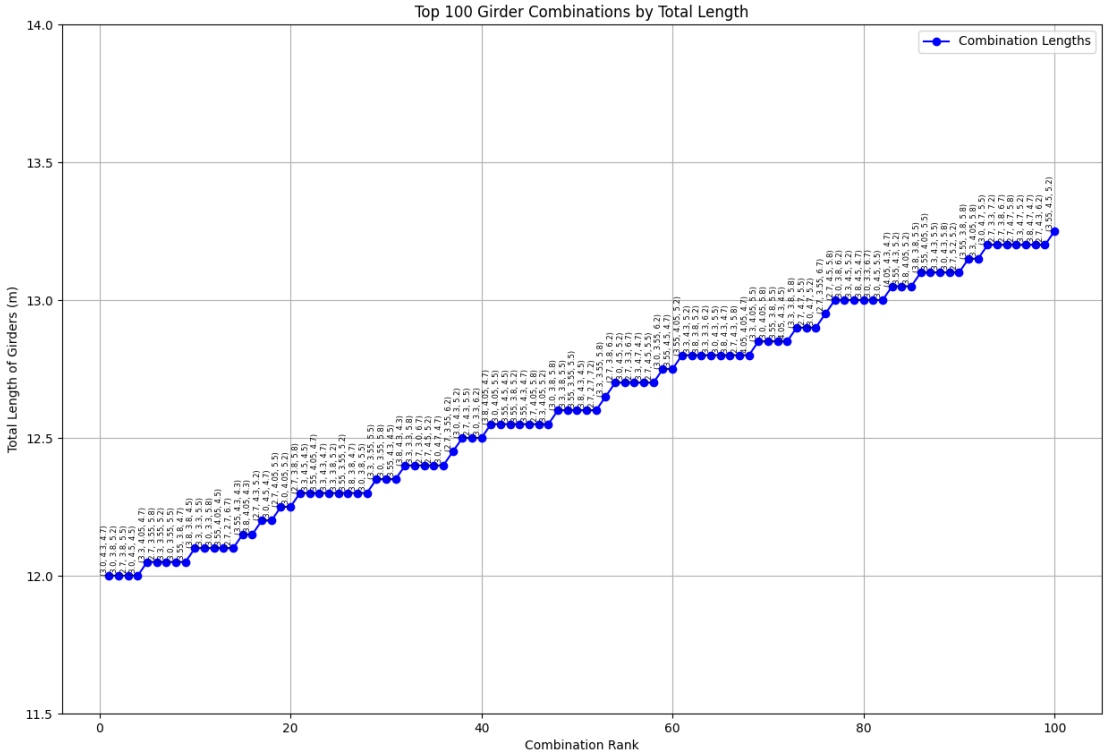

FIGURE 9 Length distribution of 100 best fitting individual module combinations.

types have been found. However, the presence of outliers beyond to the 13-meter mark emphasises the importance of a precise pre-selection when building with reused modules in order to avoid gross deviations in the resulting structure. These findings underscore the model's potential as a tool for preselection in designing with reused RC, offering a spectrum of solutions that balances geometrical precision with possible deviations.

3.2 | Load-bearing capacity-based placement using Metaheuristics

3.2.1 | Solution space and action list

It is required that all remaining solutions must be connected by means of the neighborhood structure in order to exploit the (reduced) solution space. Since all defined actions of AT1 and AT2, which built up the neighborhood, operate on module combinations and not on type combinations, it needs to be checked weather all type combinations can be generated by a trajectory of consecutive actions. Therefore, the preselected type combinations are organized as nodes with connections that represent possible actions of AT1 only (Fig. 10). The resulting graph is fully connected and thus the generated trajectories are able to exploit the entire solution space. With AT2 in addition, the graph's connectivity increases even more.

3.2.2 | Comparison of the Metaheuristics

To compare the two metaheuristics the evolution of the objective function $f(\boldsymbol{S})$ which equals the bending utilization versus the number of iterations is shown in Figure 11 for the SA (a) and TS (b). The maximum number of iterations is 3630. It is obtained from the parameters of SA in Table 2 multiplying n_{sub} and the 121 cooling steps required to reach T_{end} when starting from T_{start}.

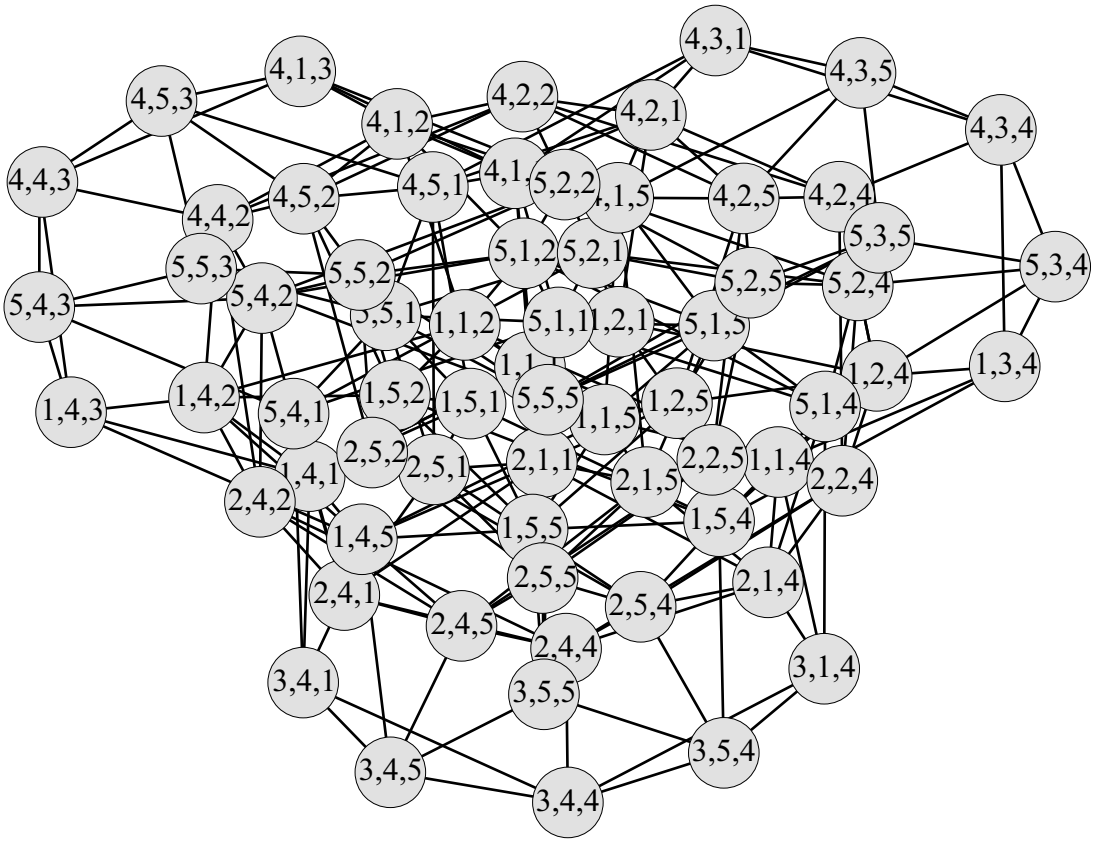

FIGURE 10 Neighborhood structure of reduced type combinations.

In case of TS the number of iterations is approximately the same. It follows from multiplication of n_N and n_{sub} according to Table 3 to 3675. These two parameters were chosen to balance the computational effort of both metaheuristics and to ensure comparability of their solution processes. To gain more search depth at each neighborhood during TS, n_{sub} has been set 2.5 times bigger than for SA. n_N follows accordingly. Each calculation is depicted as dot in the figure. The dots are colorized with respect to their compliance of load-bearing capacity. Blue dots meet the restrictions acc. to Eqs. 12 and 13, while red ones do not. The black line indicates the best solution throughout the optimization procedure, while for the dotted blue line distinction between the algorithms must be made. For SA, it corresponds to the currently accepted solution and, for TS, to the start solution of the current, examined neighborhood $N(\boldsymbol{S}_i)$.

It is evident that the SA-trajectory of $f(\boldsymbol{S}_i)$ (Fig. 11a)) initially behaves more randomly and then step by step, locates to one range of $f(\boldsymbol{S})$. Furthermore, $f(\boldsymbol{S})$ scatters more widely at first. After about 1000 iterations, 3 regions of $f(\boldsymbol{S})$ form. This is attributed to one fixed module type combination, whereby the scattering results from different module combinations of the same type.

The trajectory of $f(\boldsymbol{S}_i)$ for the TS (Fig. 11b)) is constant for each investigated neighborhood $N(\boldsymbol{S}_i)$. Peaks are observed as a consequence of generating a new start solution to diversify the search trajectory. Besides that, the scattered evaluation data mostly remains in noticeable ranges for several sequential iterations, which is reasoned in the local search behaviour throughout the whole procedure.

Both algorithms terminate with the same optimum solution, that is $\boldsymbol{S}^* = (17, 16, 61)$ and thus a corresponding module type combination of $(1, 1, 4)$. The objective function yields $f(\boldsymbol{S}^*) = 0.1188$ or a bending moment utilization of about 88% on average. In Figure 12, the utilization for $\boldsymbol{S}^*$ in contrast to an arbitrary, viable solution $\boldsymbol{S} = (3, 37, 78)$, i.e. type combination $(1, 2, 4)$, is shown with their corresponding courses of the internal forces M_{Ed} and V_{Ed}. The capacity ranges of each module M_{Rd} and V_{Rd} are highlighted in grey.

For both solutions, the maximum shear forces and the maximum hogging moments are located at the center right support. The maximum sagging moment is in the first span. However, the distribution of internal forces strongly depends on the placement and length of the individual modules and in general on the type of connections and the length in between.

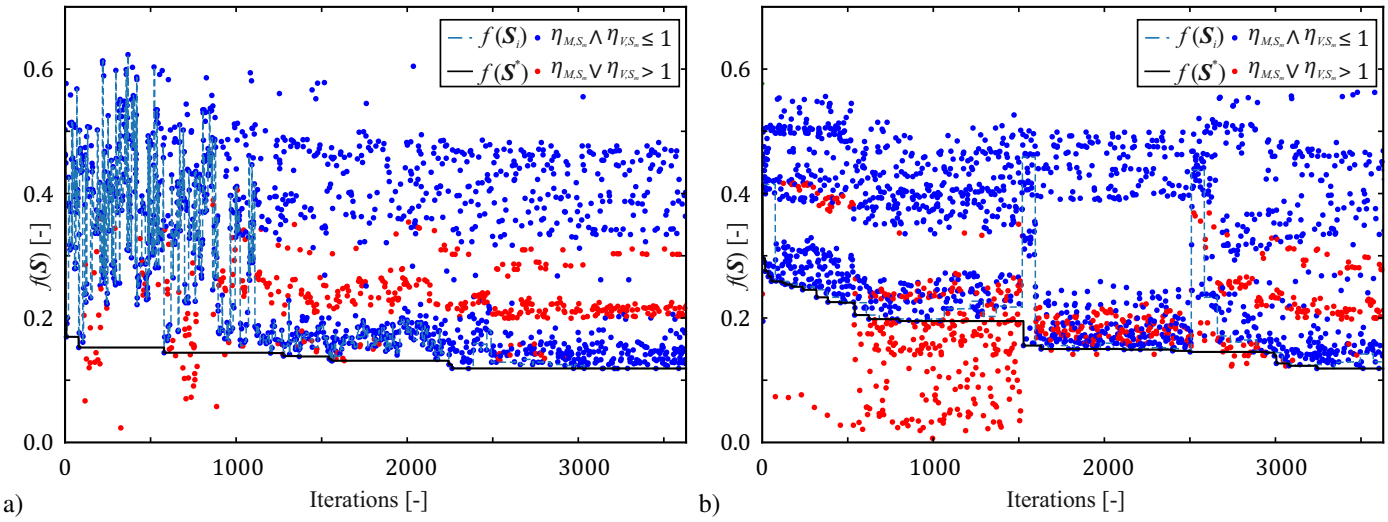

FIGURE 11 Course of the objective function for the a) SA and b) TS algorithm.

The utilizations of the single modules of $\boldsymbol{S}^*$ are 85.6%, 92.2%, and 86.6% for bending and 23%, 29%, and 19.2% for the shear force capacity. Though, the type combinations of $\boldsymbol{S}$ and $\boldsymbol{S}^*$ differ only in the center module, the bending utilization of $\boldsymbol{S}$ is 57.8% on average and thus much lower. This also holds true for the individual module utilizations of 19.4%, 23.6%, and 14.2% regarding shear. For all feasible solutions, the utilization of the bending capacity is much bigger than the corresponding utilization of the shear capacity.

The two also differ with respect to the support locations. For $\boldsymbol{S}^*$, module 17 exhibits two supports, one near the hinge between the modules 17 and 16. Another support is located in the domain of center module 16 and the last one in that of module 61 at the right. The surplus amounts to 0.11 m on each side. The arbitrary solution $\boldsymbol{S}$ has two supports in the domain of the center module 37 and one support in the domains of the other modules 3 and 78. In addition, the arbitrary solution possesses a bigger surplus of 0.79 m per side.

4 | DISCUSSION

The preselection method using ABM enables rapid exploration of possible geometric solutions, supporting decision-making and feasibility evaluation early on. As agents adjust their strategies based on past module selections, the overall outcome of actions improves over time. This iterative process of refining actions based on feedback is a fundamental characteristic of learning, allowing the model to discover more effective solutions over time. The preselection using ABM demonstrates significant potential in supporting the selection process of designing structures using reused RC modules. The ability to quickly analyse the feasibility of geometric solutions and thus make a preselection for further structural design is a valuable contribution to the holistic planning of new structures from existing modules. Further development should focus on incorporating this method into more complex design tasks, leveraging more advanced learning algorithms, and further software and workflow integration. To fully realize the potential of concrete component reuse in building design, computational frameworks need to be extended and validated for a wide range of structural typologies, such as frames, slabs, shells, and 3D spatial assemblies. This requires further research into the geometric representation and manipulation of diverse module libraries, as well as the formulation of appropriate structural analysis and optimization methods.

The implemented metaheuristics provide a tool to find an optimal placement of reuse modules with an acceptable number of numerical calculations. Thereby, the preselection of geometrically possible module type combinations drastically reduces the solution space increasing the efficacy. The best solution found has a mean utilization of 88%. The corresponding utilization of the single modules is almost evenly distributed, with one module being utilized at a level of 92 % and two beams being utilized at a level of about 86% (cf. Figure 12). Although this is a desirable result, it is conceivable to additionally adapt the optimization problem by adding restrictions, e.g. limiting the difference of utilization of the modules, to steer the optimization to equally

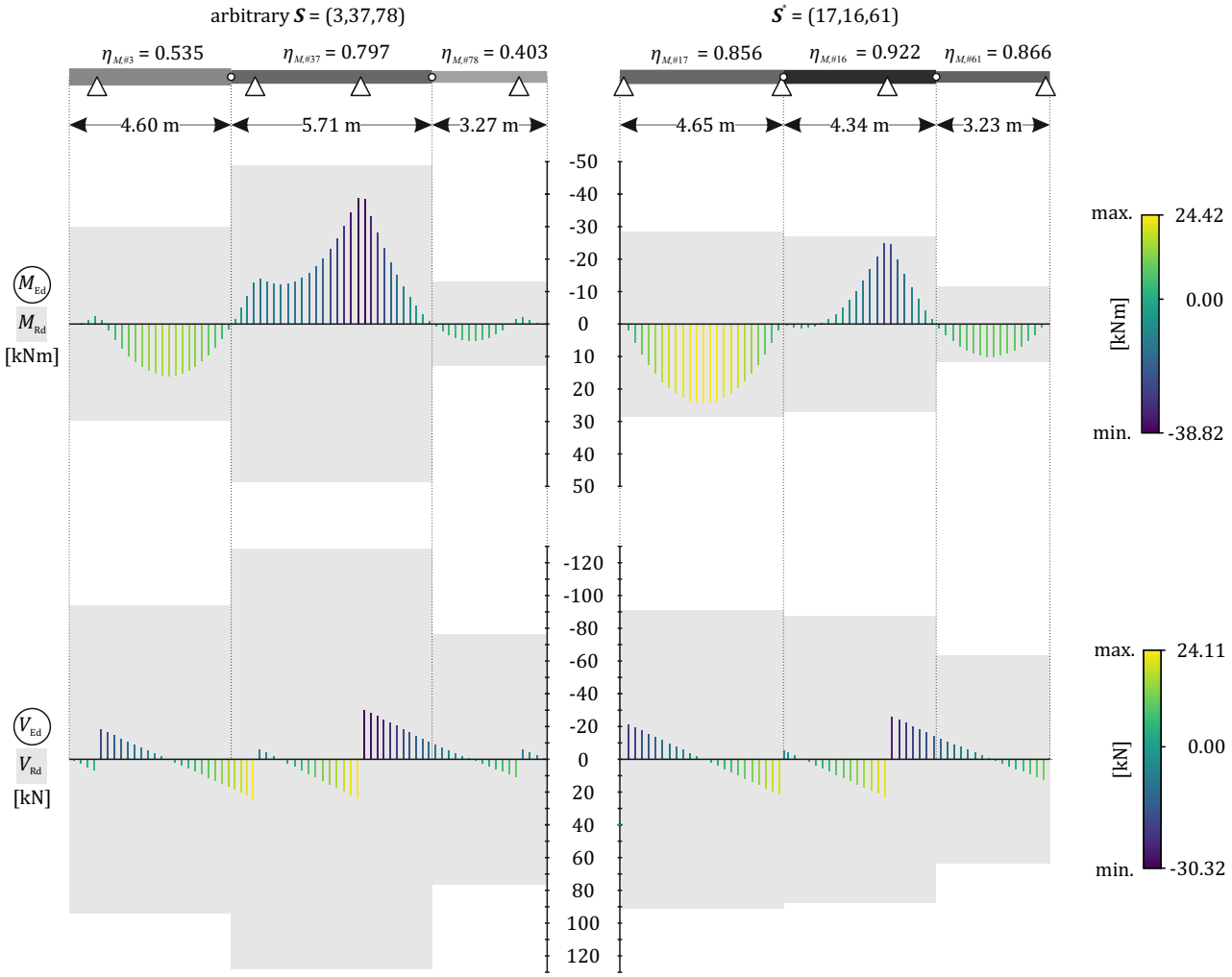

FIGURE 12 Module placement for an arbitrary solution $\boldsymbol{S}$, the best-found solution $\boldsymbol{S}^*$ with utilizations of the bending resistance for each module and curves for M_{Ed} and V_{Ed}

balanced solutions. Also, a higher utilization can be achieved when the number of modules is not restricted to 3. This increases the versatility of solutions and thus leads to a relaxation of the problem. However, if more than 3 modules are permitted the statical determination must be ensured by means of rigid connections influencing the statical system.

It can be seen that for both algorithms the best module arrangements are localized in the type combination (1,1,4). Once the search trajectory reaches that region the metaheuristics cause only small improvements of the best-known solutions due to local search. The overall range of improvement of $f(\boldsymbol{S})$ varies with the given construction kit or specific problem. To have more insight on the metaheuristic's performance or to even optimize the algorithms themselves, parameter studies and statistical evaluations should be made on a larger scale. Those were neglected in this study, due to the high computational afford that goes along with it.

The presented structural system is modelled as an idealized continuous beam. As the best-found solution shows, the arrangement contains modules with difference in height and connections are idealised as moment hinges. For actual structural designs the algorithm should be extended with a strategy to fulfill nominal measures of the floor or ceiling level. Furthermore, connections must be designed and modelled in more detail, since they affect not only the structural system but also the load-bearing capacity of the single modules edges, which is simplified in this approach as constant over its total length.

5 | CONCLUSIONS

The proposed two-stage optimization method, combining an ABM for geometric preselection and metaheuristic algorithms for maximizing structural utilization, shows promise in enabling the reuse of arbitrary reinforced concrete modules in new structures. The case study demonstrates the approach can find optimized placements for a kit of modules in a simple three-span beam configuration. The main findings are:

- By means of a geometrical preselection the solution space of module combinations is reduced to 55% of the initial solution space. Thereby, some combinations that barely met the geometric demands are still considered. Despite the preselection, the neighboring structure, which describes the possible solution space for the metaheuristics, is still connected. Thus, the metaheuristics become more efficient.
- Both metaheuristics, SA and TS, find the same best solution of the module type combination (1,1,4) with the corresponding modules (17,16,61). The reused modules are utilized about 88% on average with respect to bending. The module utilizations thereby varies between 85.6% (module 17) and 92.2% (module 16). The shear resistance is generally less utilized than the corresponding bending resistance for all calculations.
- The surplus for the best solution exhibits only 11 cm and therefore stays within the tolerance range. It also accounts to one of the best geometrical solutions that does not need additional cut offs or reworking. However, not only the surplus but also differences in height between the modules should be integrated in future enhancements of the geometrical evaluation criteria.
- For a higher utilization, hybrid approaches, i.e. combination of reused and new RC modules, could be applied, especially if the placement leads to modules with a low utilization.

In conclusion, this paper lays the foundation for a computational optimization method to enable the equivalent reuse of RC components in new buildings. Future work should focus on expanding the scope of the framework, integrating it with established design tools, and validating it on a diverse range of case studies, therefore, harnessing the full potential in supporting the design of low-carbon, circular buildings.

ACKNOWLEDGMENTS
This research was funded by the German Research Foundation DFG under Germany's Excellence Strategy - EXC 2120/1—390831618 and within the priority program 2187, grant numbers 423957563 and 423942391.

CONFLICT OF INTEREST
The authors declare no potential conflict of interests.

References

1. Eurostat . *Energy, transport and environment statistics: 2020 edition*. Statistical booksLuxembourg: Publications Office of the European Union. 2020 ed., 2020.

2. United Nations Environment Programme . 2021 Global Status Report for Buildings and Construction: Towards a Zero-emission, Efficient and Resilient Buildings and Construction Sector. https://globalabc.org/resources/publications/2021-global-status-report-buildings-and-construction; 2021.

3. Monteiro PJM, Miller SA, Horvath A. Towards sustainable concrete. *Nature materials.* 2017;16(7):698–699. doi: 10.1038/nmat4930

4. Munaro MR, Tavares SF, Bragança L. Towards circular and more sustainable buildings: A systematic literature review on the circular economy in the built environment. *Journal of Cleaner Production.* 2020;260:121134. doi: 10.1016/j.jclepro.2020.121134

5. Knoeri C, Sanyé-Mengual E, Althaus HJ. Comparative LCA of recycled and conventional concrete for structural applications. *The International Journal of Life Cycle Assessment.* 2013;18(5):909–918. doi: 10.1007/s11367-012-0544-2

6. Xia B, Xiao J, Li S. Sustainability-based reliability design for reuse of concrete components. *Structural Safety.* 2022;98:102241. doi: 10.1016/j.strusafe.2022.102241

7. Gorgolewski M. Designing with reused building components: some challenges. *Building Research & Information.* 2008;36(2):175–188. doi: 10.1080/09613210701559499

8. Küpfer C, Bastien-Masse M, Fivet C. Reuse of concrete components in new construction projects: Critical review of 77 circular precedents. *Journal of Cleaner Production.* 2023;383:135235. doi: 10.1016/j.jclepro.2022.135235

9. Fivet C. Steel, a material to reuse. *Stahlbau.* 2022;91(4):268–273. doi: 10.1002/stab.202200019

10. Küpfer C, Bertola N, Fivet C. Reuse of cut concrete slabs in new buildings for circular ultra-low-carbon floor designs. *Journal of Cleaner Production.* 2024;448:141566. doi: 10.1016/j.jclepro.2024.141566

11. Devènes J, Bastien-Masse M, Fivet C. Reusability assessment of reinforced concrete components prior to deconstruction from obsolete buildings. *Journal of Building Engineering.* 2024;84:108584. doi: 10.1016/j.jobe.2024.108584

12. Salama W. Design of concrete buildings for disassembly: An explorative review. *International Journal of Sustainable Built Environment.* 2017;6(2):617–635. doi: 10.1016/j.ijsbe.2017.03.005

13. Heckmann M, Dernbach A, Müller R, Glock C. Experimentelle Untersuchungen zu Rückbau und Wiederverwendung von Spannbetonhohldielen. *Beton- und Stahlbetonbau.* 2024;119(6):410–419. doi: 10.1002/best.202400001

14. Baghdadi A, Heristchian M, Ledderose L, Kloft H. Experimental and numerical assessment of new precast concrete connections under bending loads. *Engineering Structures.* 2020;212:110456. doi: 10.1016/j.engstruct.2020.110456

15. Bischof P, Mata-Falcón J, Burger J, Gebhard L, Kaufmann W. Experimental exploration of digitally fabricated connections for structural concrete. *Engineering Structures.* 2023;285:115994. doi: 10.1016/j.engstruct.2023.115994

16. Devènes J, Brütting J, Küpfer C, Bastien-Masse M, Fivet C. Re:Crete – Reuse of concrete blocks from cast-in-place building to arch footbridge. *Structures.* 2022;43:1854–1867. doi: 10.1016/j.istruc.2022.07.012

17. Estrella X, Muresan A, Brütting J, Redaelli D, Fivet C. RE:SLAB—a load bearing system for open-ended component reuse in building structures. *Frontiers in Built Environment.* 2024;10. doi: 10.3389/fbuil.2024.1355445

18. Huang Y, Alkhayat L, Wolf dC, Mueller C. Algorithmic circular design with reused structural elements: Method and Tool. *Conceptual Design of Structures 2021, International fib Symposium, Switzerland, September 16-18 2021.* 2021. doi: 10.3929/ethz-b-000515183

19. Gan VJ, Wong CL, Tse KT, Cheng JC, Lo IM, Chan CM. Parametric modelling and evolutionary optimization for cost-optimal and low-carbon design of high-rise reinforced concrete buildings. *Advanced Engineering Informatics.* 2019;42:100962. doi: 10.1016/j.aei.2019.100962

20. Brütting J, Senatore G, Fivet C. Form Follows Availability – Designing Structures Through Reuse. *Journal of the International Association for Shell and Spatial Structures.* 2019;60(4):257–265. doi: 10.20898/j.iass.2019.202.033

21. Brütting J, Desruelle J, Senatore G, Fivet C. Design of Truss Structures Through Reuse. *Structures.* 2019;18:128–137. doi: 10.1016/j.istruc.2018.11.006

22. Camp CV, Farshchin M. Design of space trusses using modified teaching–learning based optimization. *Engineering Structures.* 2014;62-63:87–97. doi: 10.1016/j.engstruct.2014.01.020

23. Degertekin SO, Hayalioglu MS. Sizing truss structures using teaching-learning-based optimization. *Computers & Structures.* 2013;119:177–188. doi: 10.1016/j.compstruc.2012.12.011

24. Brütting J, Vandervaeren C, Senatore G, Temmerman dN, Fivet C. Environmental impact minimization of reticular structures made of reused and new elements through Life Cycle Assessment and Mixed-Integer Linear Programming. *Energy and Buildings.* 2020;215:109827. doi: 10.1016/j.enbuild.2020.109827

25. Gonçalves MS, Lopez RH, Miguel LFF. Search group algorithm: A new metaheuristic method for the optimization of truss structures. *Computers & Structures.* 2015;153:165–184. doi: 10.1016/j.compstruc.2015.03.003

26. Alberdi R, Khandelwal K. Comparison of robustness of metaheuristic algorithms for steel frame optimization. *Engineering Structures.* 2015;102:40–60. doi: 10.1016/j.engstruct.2015.08.012

27. Stindt J, Frey AM, Forman P, Mark P, Lanza G. CO2 reduction of resolved wall structures: A load-bearing capacity-based modularization and assembly approach. *Engineering Structures.* 2024;300:117197. doi: 10.1016/j.engstruct.2023.117197

28. Forman P, Mark P. Fertigungstoleranzen von Betonfertigteilen für die modulare Bauweise. *Beton- und Stahlbetonbau.* 2022;117(5):286–295. doi: 10.1002/best.202200007

29. DIN_EN_1992-1-1 . *Eurocode_2: Design of concrete structures - Part 1-1: General rules and rules for buildings; German version EN 1992-1-1:2004 + AC:2010.* Berlin: Beuth Verlag GmbH, 2011

30. Forman P, Mark P. Interaktionsbemessung für schlanke Querschnitte aus UHPC. *Beton- und Stahlbetonbau.* 2021;116(8):607–619. doi: 10.1002/best.202100026

31. Obel M, Ahrens MA, Mark P. Settlement risk assessment for existent structures during mechanized tunneling based on uncertain data. *In: Computational Methods in Tunneling and Subsurface Engineering (EURO:TUN 2017), Hofstetter, G. et al. (eds).* 2017:405–412.

32. Fujitani Y, Fujii D. Optimum structural design of steel plane frame under the limited stocks of members. *In: Proceedings of the RILEM/CIB/ISO International Symposium, Integrated Life-Cycle Design of Materials and Structures.* 2000:198–202.

33. Bukauskas A, Shepherd P, Walker P, Sharma B, Bregulla J. Form-Fitting Strategies for Diversity-Tolerant Design. In: 2017; Hamburg, Germany:10.

34. Amtsberg F, Huang Y, Marshall DJM, Gata KM, Mueller C. Structural upcycling: Matching digital and natural geometry. In: 2020.

35. Groenewolt A, Schwinn T, Nguyen L, Menges A. An interactive agent-based framework for materialization-informed architectural design. *Swarm Intelligence.* 2018;12. doi: 10.1007/s11721-017-0151-8

36. Stieler D, Schwinn T, Leder S, Maierhofer M, Kannenberg F, Menges A. Agent-based modeling and simulation in architecture. *Automation in Construction.* 2022;141:104426. doi: https://doi.org/10.1016/j.autcon.2022.104426

37. Yang XS. *Nature-Inspired Optimization Algorithms*. Elsevier, 2014

38. Aarts E, Lenstra JK. *Local Search in Combinatorial Optimization*. Princeton, NJ: Princeton University Press, 2003

39. Maniezzo V, Boschetti MA, Stützle T. *Matheuristics*. Cham: Springer International Publishing, 2021

40. Kirkpatrick S, Gelatt CD, Vecchi MP. Optimization by simulated annealing. *Science (New York, N.Y.).* 1983;220(4598):671–680. doi: 10.1126/science.220.4598.671

41. Metropolis N, Rosenbluth AW, Rosenbluth MN, Teller AH, Teller E. Equation of State Calculations by Fast Computing Machines. *The Journal of Chemical Physics.* 1953;21(6):1087–1092. doi: 10.1063/1.1699114

42. Glover F. Future paths for integer programming and links to artificial intelligence. *Computers & Operations Research.* 1986;13(5):533–549. doi: 10.1016/0305-0548(86)90048-1

43. Gendreau M, Potvin JY. *Handbook of Metaheuristics*. 272. Cham: Springer International Publishing, 2019

APPENDIX

A DATA OF CONSTRUCTION KIT

	#	length [m]	height [cm]	$A_{s1,2}$ [cm²]	d_1 [cm]	d_2 [cm]	f_{yk} [N/mm^2]	f_{ck} [N/mm^2]	E_{cm} [MPa]	M_{Rd} [kNm]	V_{Rd} [kN]
type 1	1	4.59	20.2	3.77	3.9	3.8	500	28	32308	29.3	92.4
	2	4.69	20	3.77	4.3	4.2	500	32	33346	29.6	93.3
	3	4.60	20.1	3.77	4.0	4.1	500	31	33093	29.8	93.9
	4	4.51	21.1	3.77	3.8	4.1	500	31	33093	31.9	99.1
	5	4.48	20.2	3.77	3.8	4.1	500	31	33093	30.5	95.4
	6	4.56	20.5	3.77	3.6	4.4	500	35	34077	32.2	100.9
	7	4.42	20.0	3.77	3.8	3.7	500	27	32036	28.6	91.3
	8	4.48	19.0	3.77	4.4	4.1	500	31	33093	27.5	87.7
	9	4.57	19.7	3.77	3.7	4.0	500	30	32837	29.5	92.7
	10	4.63	20.1	3.77	4.2	4.0	500	30	32837	29.3	92.1
	11	4.43	19.4	3.77	3.7	3.8	500	28	32308	28.1	89.6
	12	4.56	20	3.77	4.3	4.2	500	32	33346	29.5	93.2
	13	4.50	19.5	3.77	4.1	3.8	500	28	32308	27.9	89.0
	14	4.36	19.8	3.77	3.8	3.8	500	27	32036	28.4	90.3
	15	4.42	19.4	3.77	4.2	4.3	500	33	33594	28.9	91.7
	16	4.34	19.9	3.77	4.2	3.5	500	25	31476	27.0	87.4
	17	4.65	20.3	3.77	3.7	3.6	500	25	31476	28.5	91.1
	18	4.57	20.4	3.77	3.8	4.0	500	29	32575	30.3	94.6
	19	4.63	20.7	3.77	4.1	3.6	500	26	31759	29.0	92.2
	20	4.68	20.3	3.77	3.9	4.5	500	37	34545	31.7	100.3
	21	5.35	24.8	5.13	4.2	3.5	500	35	34077	47.7	125.7

	22	5.43	24.4	5.13	3.9	4.0	500	39	34999	49.7	129.1
	23	5.64	24.5	5.13	4.0	3.7	500	37	34545	48.5	127.2
	24	5.67	24.3	5.13	3.7	4.2	500	43	35867	51.2	133.0
	25	5.21	24.4	5.13	3.6	3.3	500	32	33346	47.0	123.4
	26	5.33	23.9	5.13	4.3	3.7	500	36	34313	46.3	122.9
	27	5.24	23.4	5.13	3.6	4.0	500	39	34999	48.3	126.5
	28	5.62	23.5	5.13	4.3	3.8	500	38	34774	46.2	122.8
	29	5.73	24.5	5.13	3.9	4.4	500	45	36283	51.6	135.0
	30	5.37	23.1	5.13	4.0	3.9	500	39	34999	46.6	123.2
	31	5.62	24.1	5.13	3.9	4.0	500	40	35220	49.3	128.8
	32	5.28	24.5	5.13	3.5	3.8	500	38	34774	50.0	129.6
	33	5.42	24.8	5.13	4.1	4.0	500	40	35220	50.6	130.5
	34	5.70	24.0	5.13	3.9	4.0	500	40	35220	49.1	128.5
	35	5.62	23.3	5.13	4.1	4.5	500	46	36487	48.9	129.2
	36	5.62	24.0	5.13	4.2	4.1	500	41	35439	49.0	128.4
	37	5.71	23.6	5.13	4.1	4.3	500	43	35867	48.7	128.3
	38	5.38	23.7	5.13	4.0	3.7	500	36	34313	46.5	123.5
	39	5.59	25.0	5.13	4.2	4.0	500	39	34999	50.2	130.0
	40	5.38	23.5	5.13	3.6	3.6	500	35	34077	46.3	123.2
type 3	41	6.8	28.4	7.54	5.4	5	500	55	38214	84.7	167.5
	42	6.93	26.5	7.54	4.7	4.8	500	52	37659	79.6	160.5
	43	6.88	27.9	7.54	4.9	5.0	500	54	38031	84.2	166.4
	44	6.26	28.2	7.54	5.1	5.3	500	58	38751	86.2	170.3
	45	6.88	27.1	7.54	5.1	5.1	500	56	38395	82.0	164.6
	46	6.51	27.9	7.54	5.2	5.4	500	61	39271	85.7	171.1
	47	6.55	27.5	7.54	4.8	4.9	500	54	38031	83.4	165.6
	48	6.93	28.1	7.54	4.9	4.9	500	54	38031	85.1	167.4
	49	6.31	27.6	7.54	4.8	5.2	500	57	38574	84.7	168.2
	50	6.45	27.9	7.54	4.5	5.3	500	59	38926	87.2	172.0
	51	6.64	28.6	7.54	5.1	5.1	500	56	38395	86.7	170.1
	52	6.79	26.5	7.54	4.9	4.8	500	52	37659	79.2	159.9
	53	6.51	28.2	7.54	4.5	4.9	500	54	38031	86.4	169.2
	54	6.64	27.7	7.54	4.9	4.8	500	53	37846	83.4	165.2
	55	6.51	28.5	7.54	4.7	4.8	500	53	37846	86.3	168.6
	56	7.12	27.7	7.54	4.6	5.1	500	57	38574	85.6	169.5
	57	6.86	27.9	7.54	5.1	4.9	500	53	37846	83.4	165.0
	58	6.38	28.8	7.54	4.4	5.5	500	61	39271	91.5	177.8
	59	6.85	28.5	7.54	5.3	5.3	500	58	38751	86.7	170.9
	60	6.24	28.6	7.54	4.6	5.1	500	56	38395	88.3	172.0
type 4	61	3.23	16.2	1.88	3.3	2.6	500	25	31476	11.6	63.6
	62	2.88	15.7	1.88	3.1	2.8	500	28	32308	11.8	66.4
	63	3.08	15.4	1.88	3.2	2.8	500	27	32036	11.4	62.9
	64	3.08	16.9	1.88	3.1	3.0	500	30	32837	12.9	74.8
	65	2.88	16.5	1.88	3.6	3.2	500	32	33346	12.3	71.8
	66	3.05	15.5	1.88	2.8	3.3	500	34	33837	12.4	73.5
	67	2.76	15.9	1.88	3.1	2.5	500	25	31476	11.5	63.0
	68	3.18	16.0	1.88	2.8	3.2	500	33	33594	12.7	75.0
	69	3.23	16.3	1.88	2.6	3.3	500	33	33594	13.1	77.7
	70	3.09	16.6	1.88	3.1	3.0	500	30	32837	12.6	73.2
	71	2.73	17.0	1.88	3.0	2.9	500	29	32575	12.9	74.3

	72	3.26	16.3	1.88	3.2	2.6	500	26	31759	11.9	66.2
	73	2.73	16.2	1.88	2.6	2.8	500	27	32036	12.4	69.7
	74	2.85	16.5	1.88	2.6	3.1	500	31	33093	13.1	76.7
	75	2.93	15.8	1.88	3.1	3.1	500	31	33093	12.2	70.5
	76	2.95	16.6	1.88	3.2	3.1	500	31	33093	12.7	74.2
	77	2.80	16.4	1.88	2.8	3.0	500	29	32575	12.7	72.6
	78	3.27	16.7	1.88	3.0	3.2	500	32	33346	13.0	76.4
	79	2.78	15.9	1.88	3.0	3.0	500	30	32837	12.1	69.7
	80	3.15	15.3	1.88	3.1	3.3	500	34	33837	11.9	70.4
type 5	81	3.59	17.2	2.57	2.7	2.9	500	39	34999	18.2	89.3
	82	3.87	17.7	2.57	3.2	3.1	500	41	35439	18.6	92.2
	83	3.95	17.8	2.57	3.1	3.2	500	42	35654	18.9	94.5
	84	3.71	18.4	2.57	3.1	3.1	500	41	35439	19.4	97.1
	85	3.82	17.6	2.57	2.8	3.1	500	41	35439	18.7	93.4
	86	3.98	17.9	2.57	2.9	3.5	500	46	36487	19.6	100.9
	87	3.82	18.3	2.57	3.2	3.0	500	40	35220	19.0	94.2
	88	3.95	18.5	2.57	3.1	2.9	500	38	34774	19.2	94.1
	89	3.84	18.1	2.57	2.9	2.8	500	37	34545	18.8	91.5
	90	3.99	18.7	2.57	2.9	2.8	500	38	34774	19.6	96.5
	91	3.77	18.7	2.57	2.8	3.0	500	39	34999	19.8	98.2
	92	3.60	18.2	2.57	3.0	3.0	500	40	35220	19.1	94.8
	93	4.01	18.7	2.57	3.0	3.3	500	44	36076	20.1	102.6
	94	3.76	18.6	2.57	2.6	2.9	500	38	34774	19.8	97.6
	95	3.81	17.8	2.57	2.8	2.9	500	38	34774	18.8	91.8
	96	3.90	19.3	2.57	3.0	3.1	500	41	35439	20.5	103.6
	97	3.58	18.6	2.57	3.0	2.8	500	38	34774	19.3	95.1
	98	3.72	17.8	2.57	3.0	2.8	500	37	34545	18.4	89.2
	99	3.95	18.4	2.57	2.7	2.5	500	34	33837	18.7	90.5
	100	3.55	17.8	2.57	2.7	3.0	500	40	35220	19.0	94.1